

3. Crystallography

3.1 Introduction	2
3.2. Crystal Lattice and Crystal Structure	3
3.2.1 The unit cell	4
3.2.2 Basis	4
3.2.3 Crystal symmetry	6
3.3 Basic Lattice Types	7
3.3.1 Cubic lattices	7
3.3.2 Tetragonal and Orthorhombic lattices	9
3.3.3 Hexagonal lattice	10
3.3.4 Some properties of common metals	11
3.4 Close-Packed Structures	11
3.5. The Real Crystal Structure	14
3.6. Miller indices	16
3.6.1 Planes in a crystal structure	16
3.6.2 Directions in a crystal structure	18
3.6.3 Distances and angles between planes	18
3.6.4 Crystal-structure nomenclature	19
3.7. Ionic solids	20
3.7.1 The NaCl (sodium chloride) and CsCl (cesium chloride) structures	20
3.7.2 The fluorite structure	21
3.7.3 The corundum structure	22
3.7.4 Zirconia	23
3.7.5 Oxide structures with two cations	24
3.8 Experimental determination of crystal structure	2
3.8.1. X-Ray diffraction	2
3.8.2. Electron Diffraction	4
<i>Problems</i>	7
References	9

3.1 Introduction

The basic materials of nuclear reactors are metals and ceramics. As such it is important to understand the atomic arrangements in these materials. Because interatomic potentials have a long-range attraction and a short-range repulsion due to Coulomb forces, an optimal distance exists between a pair of atoms of a given type, as shown by the minimum in the interatomic potential shown schematically in Fig.6.6. The same principle applies to an ensemble of atoms arranged in a three-dimensional configuration, although the optimal distance for an ensemble of atoms is slightly different than for a pair of atoms. The thermodynamically optimal crystal structure results in a majority of the atoms interacting, which leads to denser occupation of space and to the nearest neighbor distances being close to the optimal distance. To fulfill these criteria the most stable atomic arrangement in a solid is a crystal, that is, a three-dimensional regular arrangement of the atoms in the solid. This chapter discusses the different crystal structures and their properties.

Solids (whether elemental or binary) need not retain the same crystal structure from low temperature to the melting point; for example, both iron and uranium exhibit three crystal structures, each confined to a definite temperature interval, but uranium dioxide has only one. The change from one crystal structure to another is called a *phase transformation*, as discussed in Chap.10. Such changes are the solid-solid equivalents of melting and vaporization.

The crystal structure can exert a profound effect on material behavior in the environment of a nuclear reactor, as seen from the following examples:

- Void swelling (Chap. 19) can cause unacceptable dimensional changes in structures of fast reactors or fusion reactors (but not in light water reactors). The crystal structure of the austenitic form of steel is much more susceptible to this radiation effect than that of the ferritic form of steel.
- Under fast-neutron irradiation, Zircaloy cladding of LWRs undergoes *growth* (Chap. 27) in the axial direction. This effect is due to the anisotropy of the crystal structure of zirconium.
- The utility of uranium metal as a nuclear fuel is compromised by the volume change accompanying a solid-phase transformation that occurs at relatively low temperature.
- The macroscopic properties of zirconium are directionally dependent due to crystal anisotropy and crystallographic texture, as discussed in Chapters 17 and 27.

Solid crystals exhibit one of 14 distinct crystal configurations termed the *Bravais lattices*. Each of these arrangements of atoms is characterized by a *unit cell*, which is a small group of atoms that contains the unique features of the particular lattice type. A macroscopic crystal is composed of large numbers of such unit cells periodically stacked together. The elemental and binary solids important in LWRs (and in fact the majority of materials, especially metals) exhibit only a few of the 14 possible lattice types, mainly those with the highest degrees of symmetry and the tightest packing of atoms. With one exception, these high-symmetry unit cells are parallelepipeds (all angles 90°) with side lengths denoted by a , b , and c . The exception is a structure whose unit cell is a hexagonal prism with only two characteristic dimensions. The parallelepiped with all sides of equal length (i.e., a cube) behaves in a near isotropic manner, while the other crystal structures

exhibit higher degrees of anisotropy, meaning that properties differ in the principal coordinate directions.

In binary ionic solids such as NaCl or UO₂, the distinct structures of the cations and anions are called *sublattices*.

3.2. Crystal Lattice and Crystal Structure

The stable crystalline arrangement of solids is the one with the lowest Gibbs energy. The apparent exceptions are amorphous materials, but these are metastable (occasionally with very long time constants). Since regular atomic arrangements are integral to the microscopic structure of crystals, prior to atoms being known there was little mechanistic knowledge of crystals. However some evidence of crystalline arrangements was seen in the facets of naturally-occurring minerals. This was first depicted as an ordered arrangement of building blocks as shown in Fig. 3.1.



Figure 3.1. Early postulated building blocks of materials [1]

Subsequent understanding revealed that solids are regular arrays of the constituent atoms. Taking an arbitrary point in the structure, the *lattice* is defined as the ensemble of points from which the view is exactly the same as from that arbitrary point. This means that a crystal lattice exhibits translational symmetry, meaning that any two lattice positions identified by vectors \vec{r} and \vec{r}' are related by:

$$\vec{r} = \vec{r}' + \vec{T} \quad (3.1)$$

where \vec{r} and \vec{r}' are lattice positions and \vec{T} is a translation vector such that

$$\vec{T} = n_1 \vec{a}_1 + n_2 \vec{a}_2 + n_3 \vec{a}_3 \quad (3.2)$$

where n_1 , n_2 and n_3 are integers and $\vec{a}_1, \vec{a}_2, \vec{a}_3$ are unit vectors. All points in the lattice can be reached via a lattice translation of the form given by Eq (3.1). The unit volume formed by the unit vectors is given by:

$$V = \vec{a}_1 \cdot \vec{a}_2 \times \vec{a}_3 \quad (3.3)$$

3.2.1 The unit cell

The translation vectors and its implied repetition of the unit volume leads to the concept of a *unit cell*, the building block of the material. The unit cell is a unit volume that, if systematically placed in space by successive applications of translation vectors, reproduces the full crystal structure, i.e. it will tile space in the fashion predicted by the crystal structure. Figure 3.2 shows examples of possible unit cells in a two-dimensional crystal in which the lattice points are the open circles. By translating unit cells A or A' according to Eq (3.1) using the unit vectors \vec{a}_1 and \vec{a}_2 , the complete arrangement of lattice points can be reproduced. This is also true for units B, D and E. Therefore, by definition, these are also unit cells of the lattice. Unit C, by contrast, would require the application of translation and rotation to tile space and therefore it is not a unit cell. A *primitive* unit cell contains only *one* lattice point. A is such a unit cell and contains one lattice point, as can be more easily seen by translating it to A' as shown in the figure. Each of the four atoms in A has four nearest neighbors, so A has only $4 \times 1/4 = 1$ lattice point. The same argument can be applied to B and E, but D is not primitive, as it contains two lattice points. ($4 \times 1/4$ corner atoms + $2 \times 1/2$ edge atoms).

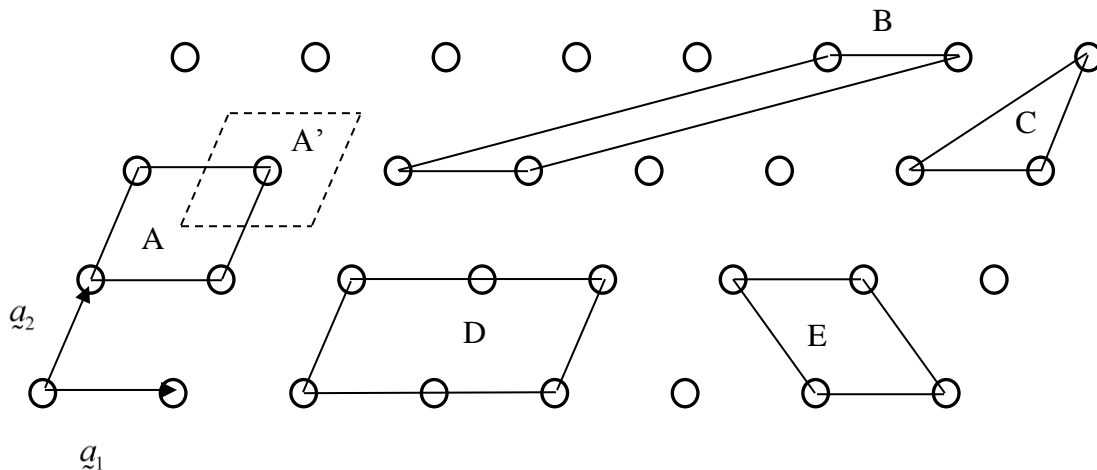


Figure 3.2. Different attempts at tiling a two-dimensional space.

3.2.2 Basis

While a lattice is a mathematical concept, the crystal structure is the actual arrangement of atoms in space. The crystal structure is formed by the application (convolution) of the *basis* to the *lattice*, so that

$$\text{lattice} \otimes \text{basis} = \text{crystal structure} \quad (3.4)$$

An illustration of the creation of a crystal structure by applying a basis to a lattice is shown in Fig. 3.3 below.

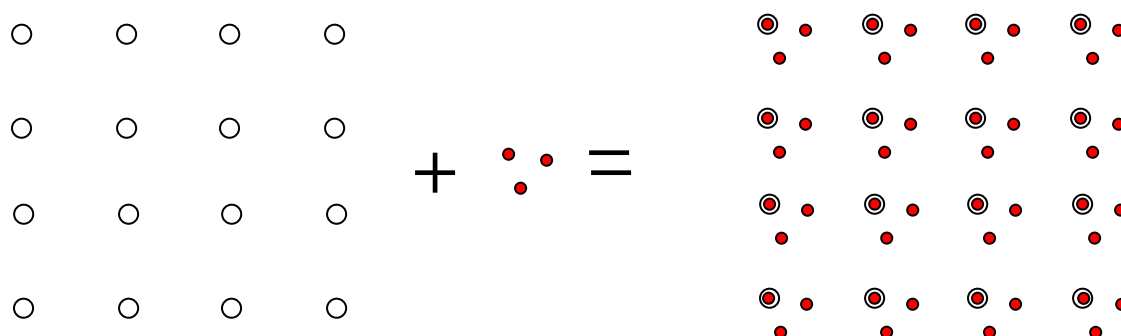


Figure 3.3 Illustration of the relationship between lattice, basis and crystal structure

Each point in the lattice on the left is associated with a basis of three atoms (shown to the right of the plus sign), forming the crystal structure on the right. Because a basis may contain an arbitrary number of atoms, a primitive unit cell may contain more than one atom, although it will always contain only one lattice point. It is also clear that for a stoichiometric compound, such as NaCl or UO_2 , the stoichiometry of the basis is by necessity equal to the overall stoichiometry of the compound.

It is possible to illustrate this more clearly using the work of the artist M.C. Escher, who created mathematically inspired prints which have well-defined two-dimensional lattices. Figure 3.4 shows interlocking black and white lizards. The unit cell can be defined by any repeating element in the structure, such as the right eye of the downward-facing white lizards or the left front paw of the rightward-facing black lizards, as illustrated by the red boxes. The lattice in this case is a grid of simple squares formed by the ensemble of arbitrary points, such as the yellow dots, (or the lizard elbows and eyes above). The basis is defined by the area delimited by the four dots.

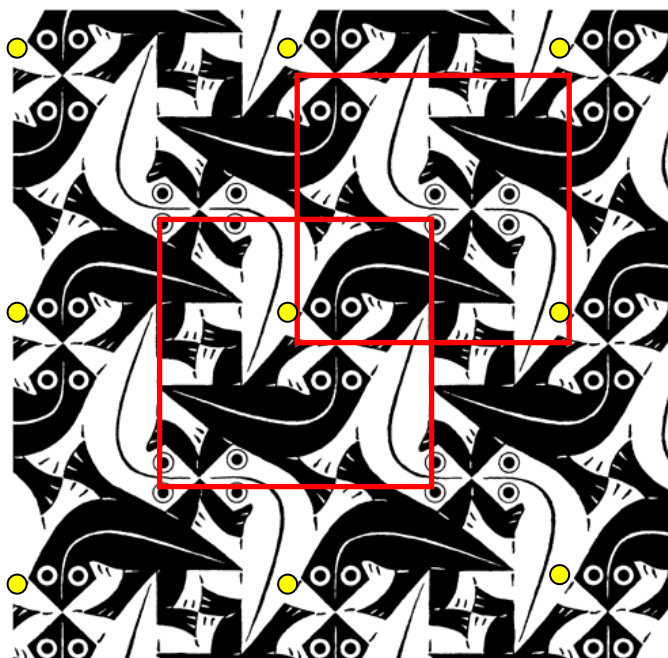


Fig. 3.4 Illustration of unit cells and basis (after M.C. Escher, *Tessellation* 104)

3.2.3 Crystal symmetry

As discussed above, and by definition, all crystals have *translational symmetry*, i.e. applying a lattice vector to any location leads to an equivalent site in the structure. Crystals also exhibit at least one axis of *rotational symmetry*, that is, rotating the structure about a given axis by a specified number of degrees takes the structure back onto itself. Crystals normally exhibit rotations of $2\pi/n$ radians around an axis, with $n=2, 3, 4$ and 6 . Crystals can also exhibit *mirror symmetry*, that is, reflecting across a plane reproduces the structure. Such elements of symmetry define a hierarchy of the crystal structure, ranging from the low-symmetry *triclinic* structure (no equal axes and all angles different) to the high-symmetry *cubic and hexagonal* structures. All these structures are defined by their elements of symmetry into the fourteen Bravais lattices as summarized in Table 3.1.

High-symmetry crystal structures are simply special cases of the low-symmetry ones. For example, a cubic system is a tetragonal structure in which the third axis is the same as the others. Most metals crystallize at room temperature in high-symmetry, high-packing-fraction structures, such as face-centered cubic (Cu, Ni, Pt, Au, Ag, Pd), hexagonal close-packed (Zr, Nb, Ti, Mg, Cd) and body-centered cubic (Fe, Cr, W, Mn, Mo, V).

Other pure elements may have more complex structures, such as U (orthorhombic) and Pu (monoclinic).

Table 3.1 Symmetry elements of Crystal structures

System	Lengths and Angles	Bravais lattices	Minimum Symmetry
--------	--------------------	------------------	------------------

			Elements
Cubic	three equal sides at right angles	Simple Body-centered Face-centered	Four threefold rotation axes
Tetragonal	three sides at right angles, two equal	Simple Body-centered	One fourfold rotation axis
Orthorhombic	three sides at right angles	Simple Body-centered Face-centered	Three perpendicular twofold rotation axes
Rhombohedral	three equal axes equally inclined	Simple	One threefold rotation axis
Hexagonal	two equal sides at 120° third side at right angles	Simple	One sixfold rotation axis
Monoclinic	three unequal sides, one not at right angles	Simple Base-centered	One twofold rotation axis
Triclinic	three different sides, three angles none 90°	Simple	None

Need illustration for some of the symmetry elements (axes?) and a problem for the rest

For example, the cubic structure, when examined along each of the four body diagonals shows the same three-fold symmetry (as shown later in the chapter) and thus it has four threefold rotation axes.

3.3 Basic Lattice Types

3.3.1 Cubic lattices

Figure 3.5 shows the unit cells of the three types of cubic crystal: the *simple cubic* (sc), the *face-centered cubic* (fcc), and the *body-centered cubic* (bcc) structures. The side length of the cube, a_o , is called the *lattice constant*.

The simple cubic lattice contains atoms at each corner of the cube.¹ The sc unit cell shown in Fig. 3.5 is a *primitive* unit cell, since it contains only *one* lattice point ($1/8 \times 8$ corner atoms). The nearest neighbor distance is a_o and each atom has six nearest neighbors.

By contrast, the bcc unit cell in Fig. 3.5 contains 2 atoms (1 center + $1/8 \times 8$ corner atoms) and thus it is a *conventional* unit cell. This representation is used more often than the primitive cell because it shows the symmetry of the lattice. The dashed line in the bcc diagram joining opposite corners of the cube and passing through the central atom is called the *body diagonal*. Its length is $\sqrt{3}a_o$. Atoms lying on this line are the most closely-spaced in this structure. The nearest-neighbor distance in bcc is thus $\sqrt{3}a_o/2$ and each atom has eight nearest neighbors. By

¹ Few elements (notably gallium) exhibit the sc structure, mainly because the packing density of atoms in this lattice is too low. However, the simple cubic structure is commonly found as a sublattice in two-component crystals.

placement of an atom at the center of the cube, the body-centered cubic structure has a higher atom density than the sc lattice. Many metals crystallize in this lattice, including α -Fe and the refractory metals tungsten, tantalum and molybdenum.

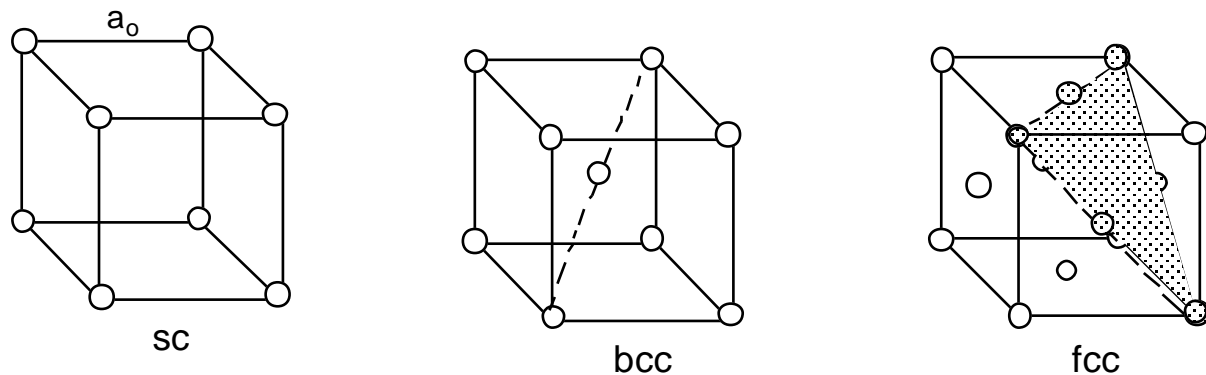


Fig. 3.5 Cubic Lattice Structures

The highest possible packing density of equal-sized atoms is achieved in the face-centered cubic lattice structure. In addition to the corner atoms, the fcc lattice contains atoms at the center of each of the six cube faces. Many common metals, including copper, gold, and nickel, exhibit fcc structures. The dashed lines joining opposing corner atoms are called *face diagonals*, which in this structure is the direction of closest packing of atoms. The nearest-neighbor distance is $\sqrt{2}a_o/2$ and each atom has twelve nearest neighbors (Fig. 3.6).

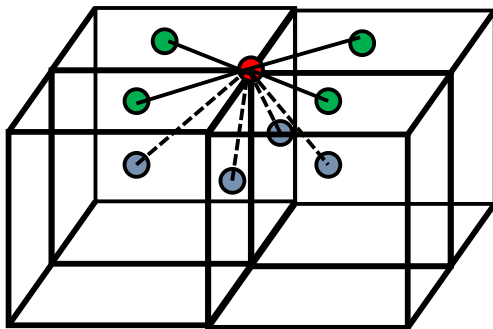


Fig. 3.6 Nearest-neighbors in the fcc lattice. The green atoms are on the middle of the upper square faces and the blue atoms on the middle of the four middle vertical squares (the 4 atoms and 4 cubes on the top are not shown for clarity- they are similar to the blue atoms)

The packing density of atoms is obtained by dividing the volume of the unit cell, a_o^3 for cubic structures, by the number of atoms in the unit cell. Atoms at the cube corners are shared by 8 contiguous unit cells, so only 1/8 of an atom is attributed to a single unit cell. Thus, the 8 corner

atoms in the cubic structure provides one atom to a unit cell. The face-centered atoms in the fcc structure are shared between adjacent unit cells, and so contribute one half an atom to each. In this structure is the direction of closest packing of atoms. The nearest-neighbor distance is $\sqrt{2}a_o/2$ and each atom has twelve nearest neighbors (Fig. 3.6).

With these rules, the atomic volumes (volume associated with each atom) of the three cubic structures are a_o^3 for the sc, $a_o^3/2$ for the bcc, and $a_o^3/4$ for the fcc.

3.3.2 Tetragonal and Orthorhombic lattices

The other two rectangular parallelepiped crystal types are the tetragonal and orthorhombic structures shown in Fig. 3.7. In the former, the end faces are square, while in the latter, all three paired sides of the parallelepiped are unequal. Both types have a “simple” version with corner atoms only. Both structures have body-centered versions, but the tetragonal lattice does not have a face-centered lattice (Example #1). Additionally, the orthorhombic lattice possesses a variant not found in either the cubic or tetragonal lattices: the end-centered type, which has face-centered atoms on only one pair of opposing faces.

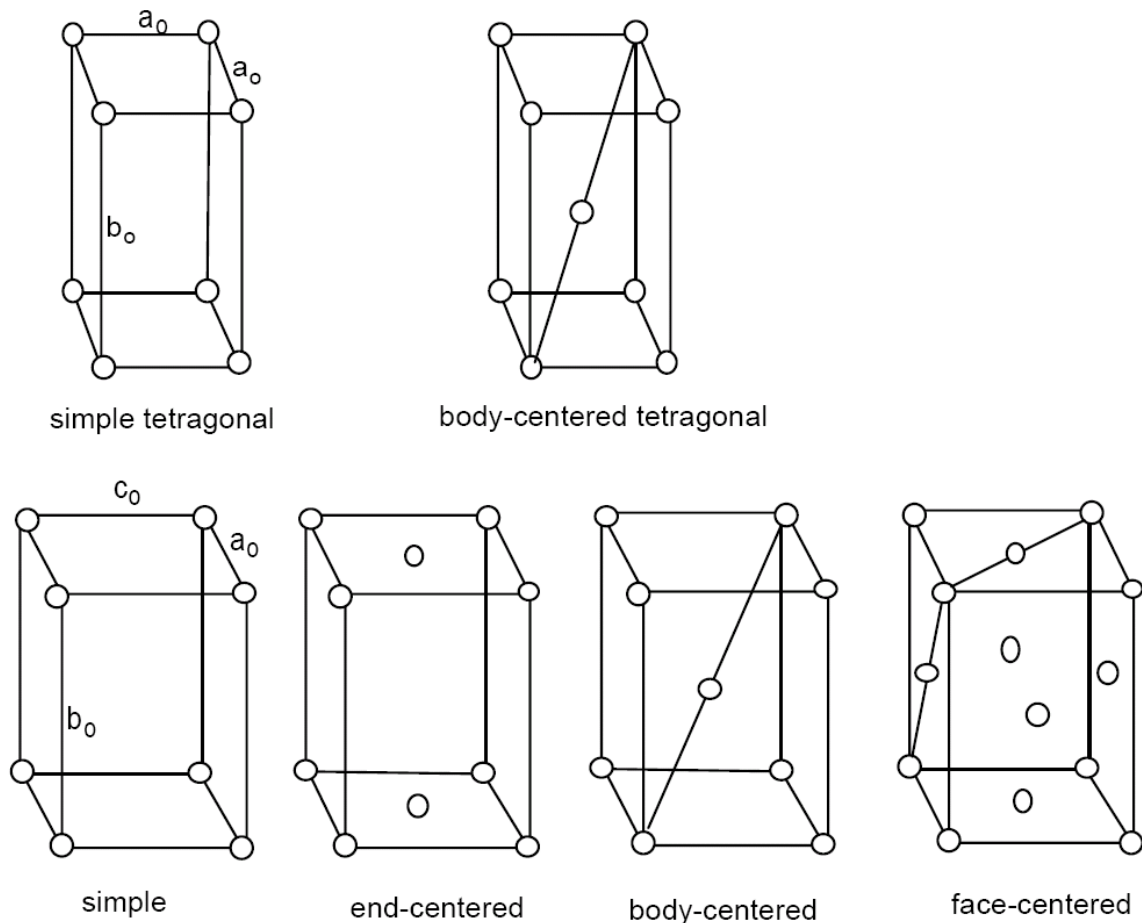
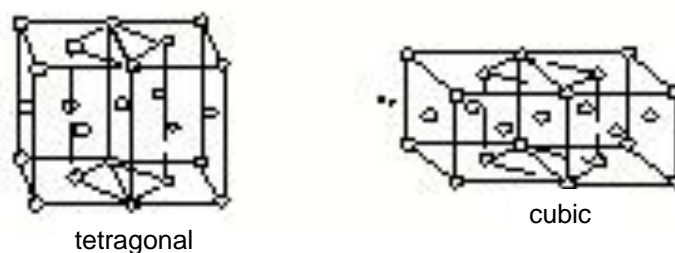


Fig 3.7 The tetragonal (top) and orthorhombic (bottom) lattice structures

Example #1 Why doesn't the tetragonal lattice system have a face-centered unit cell? Why does the cubic system have one?

The answers to these questions can be obtained by drawing two adjoining face-centered lattices of the two lattice types, as shown below. By joining the atoms in the two adjacent unit cells as shown, the left hand diagram shows that the result is a body-centered tetragonal lattice; therefore, the face-centered version is not a unique structure. Joining the same atoms in the cubic unit cells on the right, however, does not produce a body-centered cubic lattice because the length of the sides of the upper and lower squares ($a_o / \sqrt{2}$) is different from the length of the vertical edges (a_o). The new unit cell is in fact a body-centered tetragonal lattice, so that the face centered tetragonal is equivalent to a body centered tetragonal structure.



3.3.3 Hexagonal lattice

The last of the common crystal structures is the *hexagonal close-packed (hcp)* crystal structure, whose unit cell is shown in Fig. 3.8. The low-temperature form of the important nuclear material zirconium has this structure. The atomic configuration consists of alternating planes of atoms seen as the upper and lower planes in Fig. 3.8. The atoms located between these planes are centrally placed in alternating pie-shaped wedges of the hexagonal prism. Although not obvious from Fig. 3.8, these atoms form a planar structure identical to that of the upper and lower planes but offset so that its atoms nestle in the center of the equilateral triangles formed by the atoms of the adjacent planes. This structure has two characteristic lengths: the distance between the upper and lower planes, denoted by the letter c , and the length of the spokes emanating from the central

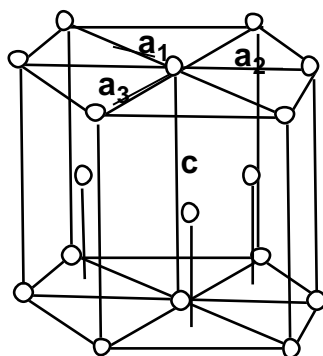


Fig. 3.8 The hexagonal crystal structure

atom, designated by a_1 , a_2 and a_3 , although all three are the same magnitude, a . Thermal, mechanical, and transport properties in the a and c directions are very different. The horizontal planes in the structure (upper, middle and lower) are termed *basal planes*, and the six vertical faces are called *prism planes*.

3.3.4 Some properties of common metals

Table 3.2 lists several structure-related properties of metals commonly found in LWRs: zirconium and two types of iron: the bcc structure of pure iron; and the fcc structure of steel. The atomic volume (Ω , nm³/atom) is related to the macroscopic properties by:

$$\Omega = \frac{M}{\rho \times N_{Av}} \times (10^7)^3 \quad (3.5)$$

where ρ is the density in g/cm³, M is the element's atomic weight and $N_{Av} = 6.023 \times 10^{23}$ atom/mole is Avogadro's number. The numerical factor converts cm³ to nm³. The entries in the last column of Table 3.2 are based on this equation.

Table 3.2 Properties of some common metals

metal	structure	Atomic wt. (g/mole)	Density (g/cm ³)	Lattice constant, (nm)	Atomic volume, (nm ³)
iron	bcc	56	7.9	0.287	0.0117
copper	fcc	63.5	8.96	0.361	0.0117
zirconium	hex	91	6.5	a = 0.323 c = 0.514	0.0232

For elemental cubic structures, the atomic volume can be related to the lattice constant by:

$$\Omega = a_o^3 / n \quad (3.6)$$

where n is the number of atoms in the unit cell of Fig. 3.5 ($n = 1$ for sc, $n = 2$ for bcc and $n = 4$ for fcc). Equations (3.5) and (3.6) both produce atomic volumes which should agree exactly except for lattice defects, discussed in the following chapters. (Example #4)

3.4 Close-Packed Structures

The fcc lattice on the right of Fig. 3.5 and the hcp lattice of Fig. 3.8 are more closely related than they appear from the diagrams. If the atoms from the adjacent unit cell in the fcc diagram of Fig. 3.5 were included, the shaded atoms would be seen to be part of the same hexagonal (basal) plane as that in Fig. 3.8. The two shaded planes in the fcc structure depicted in Fig. 3.9a are close packed planes (seen in Fig. 3.9b), similar to the basal planes in the hcp structure shown in Fig. 3.9c. This is because for clarity, the atoms in Figs. 3.5 - 3.9a have been drawn as small circles occupying only the corners of the structures. In real crystals, however, the atoms (or ions) are packed together until their electron clouds overlap. If regarded as hard spheres, the atoms in

crystals “touch” each other, as seen in Fig. 3.9b. The arrangement shown in Fig. 3.9b is the maximum packing density of spheres on a plane, which accounts for the designation *close-packed plane* for this planar configuration.

Example #2 If all circles touch, what is the fraction of the total surface area occupied by the atoms in the close-packed plane?

The side length in the equilateral triangle in Fig. 3.9b is half of a face diagonal, or $a_o/\sqrt{2}$. The area of this triangle is $\sqrt{3}a_o^2/8$ and it includes $1/2$ of an atom plus the associated open space. The total surface area per atom is thus $\sqrt{3}a_o^2/4$. The radius of the touching atoms is one quarter of a face diagonal, or $a_o/2\sqrt{2}$. The area of the atom, excluding the associated open space, is $\pi a_o^2/8$. The atoms therefore occupy $\pi/2\sqrt{3} = 90.7\%$ of the surface.

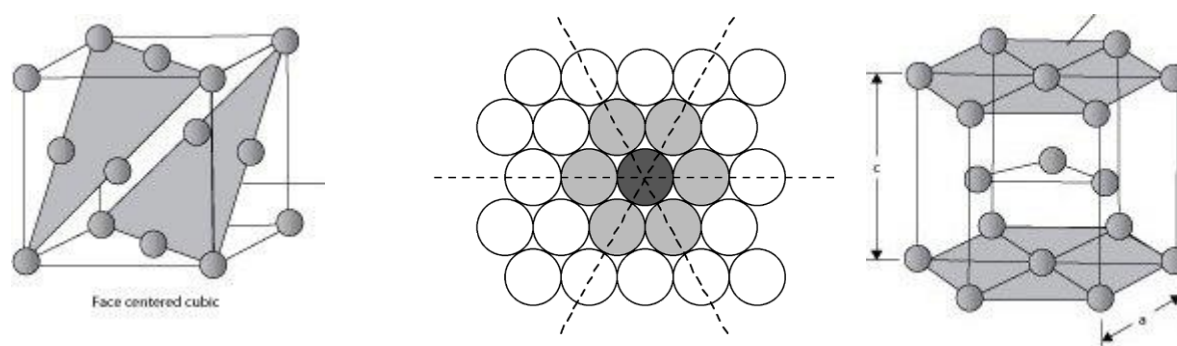


Fig. 3.9 The close-packed plane. (a) in the fcc lattice (b) drawn as touching atoms (c) in the hcp lattice

The fcc and hcp structures can be created by stacking close-packed planes on top of each other. This plane is shown in Figure 3.9b and on edge in the left of Fig. 3.10. The next plane is placed on top of the first so that its spheres nestle in the depression (i.e., the empty spaces) formed by trios of atoms in Fig. 3.9b. This arrangement gives the highest-density, or closest-packed, three-dimensional lattice. In this arrangement, whether fcc or hcp, each atom touches 12 nearest neighbor atoms. It is the placement of the third close-packed plane that distinguishes the fcc and hcp structures. There are

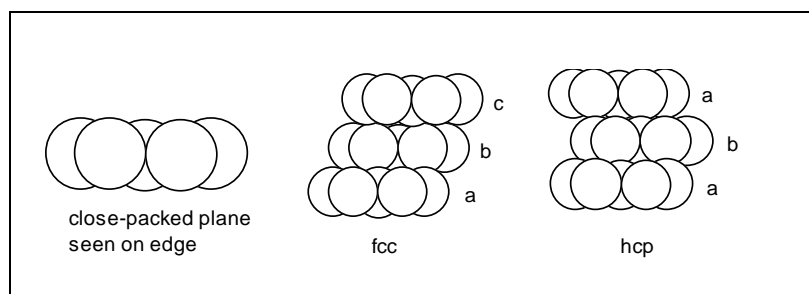


Fig. 3.10 Stacking sequences of close-packed planes in the fcc and hcp lattices

two ways of placing this third plane so that it fits into the depressions of atom trios in the second plane. One way places the third plane in a position distinct from the first and second planes; the other is directly over the first plane. The former gives the fcc lattice, which can be constructed by stacking close-packed planes in an $abcabc\dots$ sequence. The hcp lattice exhibits a stacking sequence $ababab\dots$. Each atom in both lattices have 12 nearest neighbor atoms separated from the central atom by half of an fcc face diagonal, or $a_o/\sqrt{2}$. The three contiguous atoms in one plane and the atom in the next plane that sits in the depression of the three form a regular tetrahedron with side length $a_o/\sqrt{2}$. The distance between the close-packed planes in the fcc and hcp structures is the height of this tetrahedron, which a bit of solid geometry shows to be $a_o/\sqrt{3}$.

Example #3 What fraction of the total volume in the fcc and hcp lattices is occupied by the atoms if the nearest neighbors touch as hard spheres?

As shown earlier, the fcc unit cell contains 4 atoms and occupies a total volume of a_o^3 . Each atom, with radius $a_o/(2\sqrt{2})$, has a volume of $(4/3)\pi[a_o/(2\sqrt{2})]^3$. This volume, divided by the total volume associated with each atom ($a_o^3/4$), gives a fraction $\pi/(3\sqrt{2}) = 0.74$ of the space occupied by atoms. Or, the void fraction in the close-packed structures is 0.26. All other crystal lattices have higher void fractions when packed with spherical atoms.

Example #4 What is the volume per atom in the hcp structure?

In the hcp unit cell of Fig. 3.8, the volume of the six triangular prisms that make up the unit cell are to be determined. The area of the equilateral triangles that form the base of the prisms is

$\frac{1}{2}(\sqrt{3}/2)a \times a$, where a is the side length of the triangle. The area of the hexagonal cross section of the unit cell is 6 times this value, or $3\sqrt{3}/2 a^2$. A bottom triangle and the atom in the middle plane that sits

on top of it form a regular tetrahedron whose height is $\sqrt{2/3} \times a$. The height of the unit cell in Fig. 3.8 is

twice this value, or $c = 2\sqrt{2/3} \times a$. The volume of the unit cell is $(3\sqrt{3}/2 a^2)(2\sqrt{2/3} \times a) = 3\sqrt{2} a^3$.

Since the unit cell contains 6 atoms, the volume per atom in the hcp structure is:

$$\Omega_{hcp} = a^3 / \sqrt{2} = 0.023 \text{ nm}^3 \quad (3.5b)$$

The radius of hard-sphere atoms in the hcp crystal is $\frac{1}{2}a$, or the volume per atom is $(\pi/6)a^3$. When this is divided by Ω_{hcp} , the fractional occupancy of the available volume is $\pi/(3\sqrt{2})$, which is identical to the value obtained in Example #3 for the fcc structure. This is expected since both crystals are close-packed.

Note that the example above is only valid for the ideal c/a ratio of 1.633. Real hcp crystals often deviate from the ideal value, for example Zr has a c/a ratio of 1.593. In that case the packing fraction will be lower than 0.74.

3.5. The Real Crystal Structure

As implied by Fig.3.3., in all of the lattice types discussed until now, the locations of the atoms defined the structure of the crystal, i.e. there is a one to one correspondence between the lattice points and atoms. However, this need not be so; the points in space that determine the lattice type need not be occupied by atoms (Fig. 3.3). A prime example of this disjunction of lattice and atoms is the *diamond structure*, which is characteristic of the diamond form of carbon and the semiconductor elements germanium and silicon. These group IV elements form four covalent bonds with nearest neighbors. These covalent bonds act as additional constraints on the crystal structure; therefore, they cannot crystallize in the common crystal structures of the other elements, in which the numbers of nearest neighbors are twelve (fcc and hcp), eight (bcc) and six (sc).

The conventional unit cell of the diamond structure is shown in Fig. 3.11a. This structure can be viewed either as i) an fcc framework (open circles) with four atoms internal to the unit cell (filled circles); or ii) regular tetrahedrons formed by opposite corners of the small cubes, half of which have a central atom. Neither of these views constitute a fundamental lattice structure. Reduction of the diamond structure to one of the basic types discussed previously is achieved by considering the structural unit that replaces a single atom by a dumbbell consisting of one open circle and one filled circle at $\frac{1}{4}$ of a body diagonal away. In Fig. 3.11a, this basis is represented by the open circle at the lower left-hand corner of the heavy small cube and the filled circle to its right.

As shown in Fig. 3.11b, the alternative representation is constructed of these atom pairs with the lattice type defined by the crosses midway between them. The diamond structure is therefore not an independent lattice type. Rather it exhibits an fcc *space lattice* with a *basis* of two, the latter denoting the two atoms associated with each point of the space lattice.

Alpha uranium also exhibits a structure with atoms associated with, but not on, the lattice points (see problem 3.1).

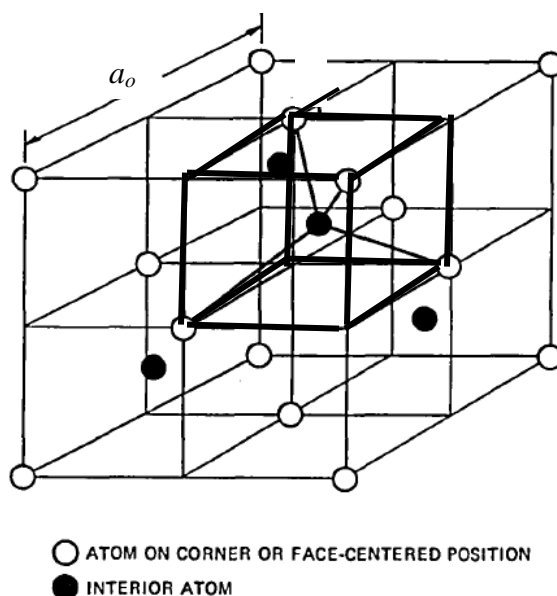


Fig. 3.11a The conventional unit cell of the diamond structure

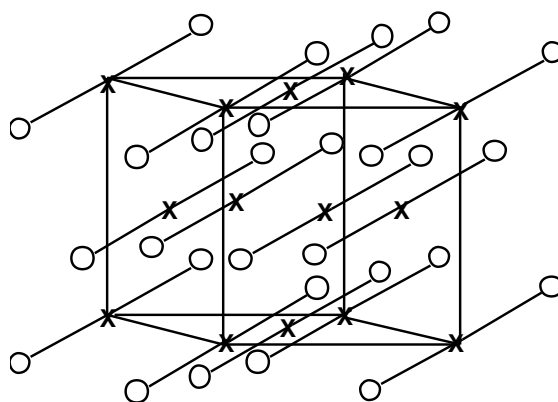


Fig. 3.11b: The diamond structure represented as an fcc space lattice with a basis of two

The other form of solid carbon, graphite, is a layered structure similar to the hcp lattice of Fig. 3.8. However, as shown in Fig. 3.12, the central atom of the basal-plane hexagons is missing. The reason for this is the nature of the carbon-carbon electronic bond. In diamond, carbon atoms are joined by *single* bonds, meaning that one electron from each atom is shared with one from an adjacent atom. In graphite, instead of the tetrahedral bonding characteristic of diamond, the four electrons from each carbon atom form three bonds with three neighbors in the basal plane. The three bonds are each $1/3$ double-bond character and $2/3$ single-bond character. Because the bonding electrons are consumed in the basal plane interactions, interplanar bonding in graphite is very weak (this is what makes graphite a good lubricant). The properties of graphite are very different in the a and c directions. Also, the weak interplanar bonding makes the c/a ratio larger than that in the hcp structures of most metals.

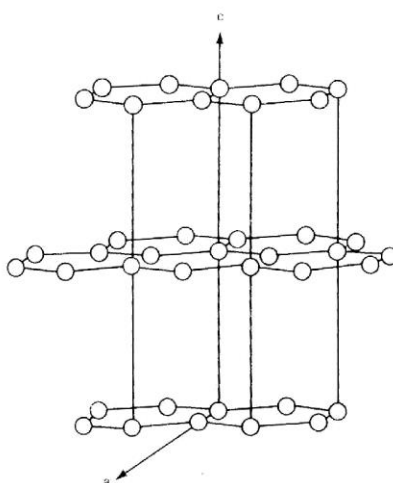


Fig. 3.12 The graphite structure

3.6. Miller indices

Analysis of the properties of crystalline solids requires a method of identifying atomic planes and directions in the lattice. The term “close-packed” has been used to describe the atomic planes in Figs 3.9 and 3.10. However, there are many more planes in the various structures, and word descriptions of these are obviously impossible. Similarly, the terms “body diagonal” and “face diagonal” have been applied to directions in cubic crystals. Designating the many other directions calls for a more concise labeling technique.

3.6.1 Planes in a crystal structure

A general method for designating planes starts with a coordinate system whose unit vectors a , b , and c (called *crystal axes*) are equal to the lengths of the sides of the unit cell and point in the directions of these sides (see Fig. 3.13). The recipe for designating a plane is as follows:

1. Pick an origin at a lattice point that is not in the plane to be designated
2. From this origin, draw the crystal axes. Determine how many multiples of the unit lengths of these vectors are required to reach the plane in question. These multiples are designated as f_a , f_b , and f_c .
3. Take the reciprocals, $f_a^{-1}, f_b^{-1}, f_c^{-1}$
4. Reduce the reciprocals to the set of smallest integers and enclose them in parentheses (hkl). These are the Miller indices of the plane.

Application of the Miller index method to the three principal planes in the cubic crystal system is illustrated in Fig. 3.13. For clarity, the atoms in the structure are omitted and the planes in question are drawn in each cube. The origin of the lattice vectors is placed at the lower left hand corner of the cube.

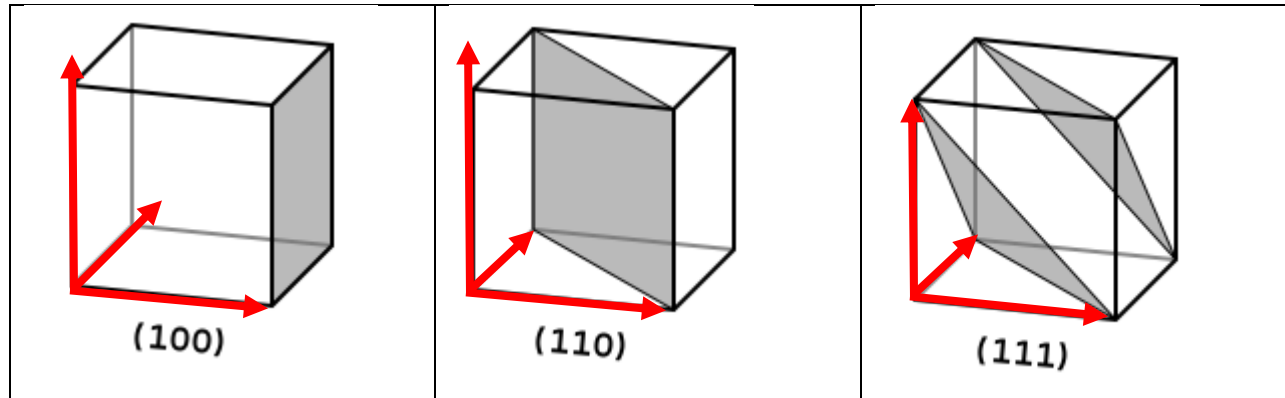


Fig. 3.13 Principal planes in the cubic lattice

- The shaded plane in the left-hand cube intersects the a lattice vector at one unit. The plane is parallel to the other two lattice vectors. Therefore, $f_a = 1$, $f_b = \infty$ and $f_c = \infty$. Taking the reciprocals gives $f_a^{-1} = 1$, $f_b^{-1} = 0$, $f_c^{-1} = 0$. These form the smallest integers, so the Miller indices of the plane are (100).
- In the center cube, both a and b intersect the shaded plane at unit lengths and c is parallel to the plane. For this case, $f_a = 1$, $f_b = 1$ and $f_c = \infty$, and $f_a^{-1} = 1$, $f_b^{-1} = 1$, $f_c^{-1} = 0$. The shaded plane is the (110) plane in Miller index notation.
- The shaded plane in the right-hand cube is intersected at unit values of all three crystal axis vectors, and is denoted by (111).

The system employing three crystal axis vectors can be applied to any lattice type. For the hexagonal structure, however, the Miller index system is slightly modified to reflect the hexagonal symmetries of this lattice. In addition to the c axis, three other unit vectors are the sides of the equilateral triangles that constitute the basal planes in Fig. 3.8. These side lengths are all equal to a , but in the Miller index system, they are labeled a_1 , a_2 and a_3 . The indexing method is identical to that described above for the cubic system except for the inclusion of a redundant unit vector. With the origin at the center of the bottom hexagon in Fig. 3.8, the intersections of the upper hexagon with the unit vectors is $f_{a_1} = \infty$, $f_{a_2} = \infty$, $f_{a_3} = \infty$, $f_c = 1$. Taking reciprocals, the Miller index of the basal plane is (0001). Starting from the front plane in Fig. 3.8 and moving clockwise, the six prism planes in the hexagonal structure are $(\bar{1}010)$, $(0\bar{1}10)$, $(1\bar{1}00)$, $(10\bar{1}0)$, $(01\bar{1}0)$ and $(\bar{1}100)$. The notation $\bar{1}$ means -1 , which results from the Miller index recipe when the unit vector points away from the plane to be designated. The general Miller index for the hexagonal structure is $(hkil)$. To account for the extra lattice vector, $h + k + i = 0$.

3.6.2 Directions in a crystal structure

A modified version of the Miller index method for naming planes is applicable to designating directions in a crystal. From an origin on a lattice point, the line is drawn in the desired direction and terminates at an arbitrary point, whose coordinates are described as n_a , n_b and n_c multiples of the lattice vectors. These numbers are reduced to the lowest set of integers i , j , and k , and enclosed in brackets to give the Miller indices for the direction as $[hkl]$ (or $[hkil]$ for hexagonal lattices)

Example #5: What are the directions perpendicular to the shaded planes in Fig. 3.13?

The origin is chosen as lower front left hand corner of the cubes.

- From this origin, the line perpendicular to the (100) plane in the first cube is coincident with the a lattice vector. The end point is chosen as the intersection of this direction with the (100) plane. The coordinates of this point are $n_a = 1$, $n_b = 0$, $n_c = 0$, so the direction is $[100]$.
- Using the same origin, the direction perpendicular to the (110) plane in the center cube is one half of a face diagonal. The intersection of this plane with the face diagonal occurs at lattice vector units of $n_a = 1/2$, $n_b = 1/2$ and $n_c = 0$. Multiplying by 2 to convert to integers gives the Miller index of $[110]$. This is the direction of the face diagonal in the cubic system
- The perpendicular to the (111) plane in the right hand cube in Fig. 3.13 is the body diagonal starting from the origin. To find this direction, it is not necessary to terminate the line on the (111) plane. The line is continued to the opposite corner of the cube where the coordinates are $n_a = n_b = n_c = 1$, giving $[111]$ for the Miller index.

The above example suggests the general rule that *in cubic crystals, directions and the planes perpendicular to them have the same Miller indices*. This is only true in general for the cubic system; in other crystal structures this is true only for a few select planes. The rule for assigning the Miller indices of directions with those of the planes perpendicular to them does not apply to the tetragonal or orthorhombic crystal structures, or any other lattice types with lower degrees of symmetry. For example in the hexagonal lattice (Fig. 3.8), the lattice direction is perpendicular to the basal plane but to no others.

3.6.3 Distances and angles between planes

The distance between crystal planes is the quantity most often measured using x-ray diffraction to determine crystal structure. In a cubic crystal the distance between successive (100) planes is simply a_o . These are the most widely-spaced planes in the structure. The distance between (110) planes can also be visualized by looking at the cube from the z direction, where it is found that it is one half the face diagonal or $a_o/\sqrt{2}$. In general for cubic lattices the distance between (hkl) planes is:

$$d_{hkl} = \frac{a_o}{\sqrt{h^2 + k^2 + l^2}} \quad (3.7)$$

The angles between planes are also of interest. For the cubic system the angle between $(h_1k_1l_1)$ and $(h_2k_2l_2)$ is:

$$\phi = \cos^{-1} \left[\frac{h_1 h_2 + k_1 k_2 + l_1 l_2}{\sqrt{(h_1^2 + k_1^2 + l_1^2)(h_2^2 + k_2^2 + l_2^2)}} \right] \quad (3.8)$$

for the other systems the interplanar distances and formulas can be found in [2].

3.6.4 Crystal-structure nomenclature

The systematization of crystal structures and their elements of symmetry, as well as the actual atomic positions, represent a rich trove of experimental data that has been painstakingly gathered using primarily x-ray diffraction.

Crystals are uniquely defined by their *space group* listed in the International Tables for Crystallography[3]. It has been shown that 230 different space groups exist and although a complete description of the space groups is beyond the scope of this book, it is useful to note that the tables list the so-called Wyckoff positions which define the positions of the atoms in the unit cells for a given structure. The unit cells in the sections above are very simple and can be described by the positions of a couple of atoms. For more complex crystals the unit cells may be bigger and involve a larger number of formula units, and the complete listing in the tables is essential.

The space group description includes the essential symmetry elements of the structure and could be used as a unique descriptor of the structure. In practice researchers use other conventions including the Pearson and Strukturbericht conventions. In addition, the structures may have special nicknames from tradition. For example, the most common intermetallic precipitates formed in Zircaloy have the compositions $\text{Zr}(\text{Cr},\text{Fe})_2$ or $\text{Zr}_2(\text{Ni},\text{Fe})$. The $\text{Zr}(\text{Cr},\text{Fe})_2$ precipitates in particular have been described as Laves phases, after the discoverer of this archetypical structure[4]. These phases maximize the packing fraction for atoms of different sizes and with a given ratio. Two variants exist and they are commonly known by their Strukturbericht designation, C15 (cubic phase) or C14 (hexagonal phase); a third high temperature hexagonal phase exists, designated as C36. The C14 phase is also referred to as MgZn_2 type (after the original compound) and the C15 phase as MgCu_2 type.

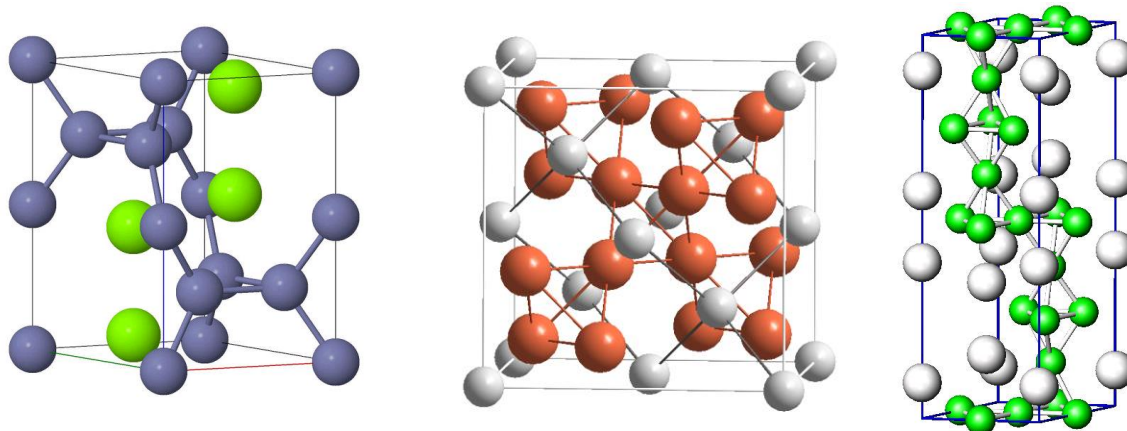


Figure 3.14: Laves Phase structures: (a) C14 hcp MgZn_2 type, (b) C15 fcc MgCu_2 type (c) C36 MgNi_2 type structure.

3.7. Ionic solids

Many technologically-important solids consist of two elements. Naturally occurring minerals often contain three or more elements. The two-component solids are combinations of electropositive elements from the left side of the periodic table and electronegative elements from the right side. As neutral elements, the former possess 1 –3 electrons in their outer electron shell and the latter lack 1 or 2 electrons in their outermost orbital. As a result, transfer of the electrons between the two neutral elements is energetically favorable. The resulting compound consists of positive ions called *cations* ($\text{M}^{z_M^+}$) and negative ions termed *anions* ($\text{X}^{z_X^-}$). Both the formula of these *ionic solids*, M_jX_k , and their crystal structures are determined by the charges (valences) of the cations and anions. Electrical neutrality of the ionic solid requires:

$$j \times z_M = k \times z_X.$$

Much information is available by knowing the crystal structure and *lattice parameter*. For example, the density of the material can be calculated from the composition and size of the unit cell.

Crystal structures of two-component ionic solids are best viewed as interlaced *sublattices* of cations and anions. Each sublattice is one of the simple types treated earlier in this chapter. For minimum crystal energy, the structures are restricted to those in which all cation nearest neighbors are anions and vice versa. This condition maximizes the Coulomb attraction of the two oppositely-charged species. The lattice type is named for a common compound that exhibits the particular structure.

3.7.1 The NaCl (sodium chloride) and CsCl (cesium chloride) structures

The NaCl structure is shown in the left hand diagram of Fig. 3.15. This lattice type consists of two intermingled sublattices of the fcc type, and is characteristic of cations and anions of the

same valence. Examples of this structure include NaCl (unit-valence cation and anion), MnO (divalent ions) and UC (tetravalent elements).

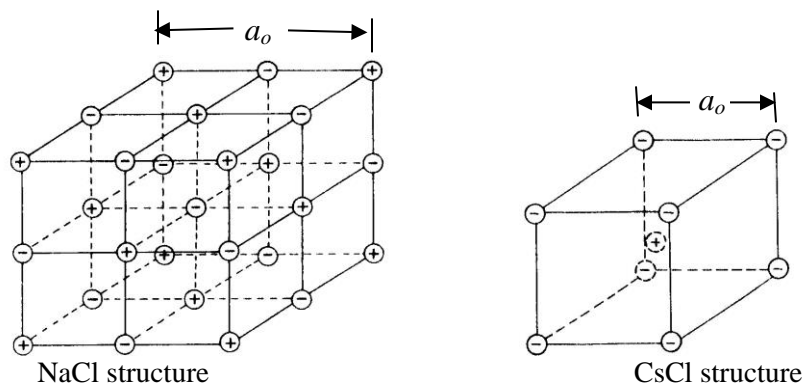


Fig 3.15 Lattices formed by compounds of equal-valence ions

The other common lattice formed by compounds with equal-valence cations and anions is the CsCl structure depicted on the right of Fig. 3.15. This structure consists of two interlaced simple cubic sublattices. Whether an MX solid exhibits the NaCl or CsCl structure depends on the relative sizes of the anions and cations and on the interatomic forces responsible for formation of the solid.

3.7.2 The fluorite structure

The nuclear fuel uranium dioxide (UO_2) crystallizes in the *fluorite* structure, named after the prototype CaF_2 , a naturally occurring mineral. In this ionic solid, the cation valence is twice the anion valence. Two views of this structure are shown in Fig. 3.16. The U^{4+} ions form an fcc sublattice that meshes with a simple cubic O^{2-} sublattice. The left hand version shows that U^{4+} ions occupy every other cube formed by the anions. Joining these four U^{4+} ions creates a regular tetrahedron (red lines) with an oxygen ion in its center.

The right hand drawing shows the structures of the two sublattices more clearly. One of the major advantages of UO_2 as a nuclear fuel is the stability of its fluorite structure up to the melting point of 2860°C . The oxygen ions that accord UO_2 its great stability serve no nuclear purpose. However, they occupy space and result in the undesirable low uranium density of UO_2 , which is one-half that of U metal.

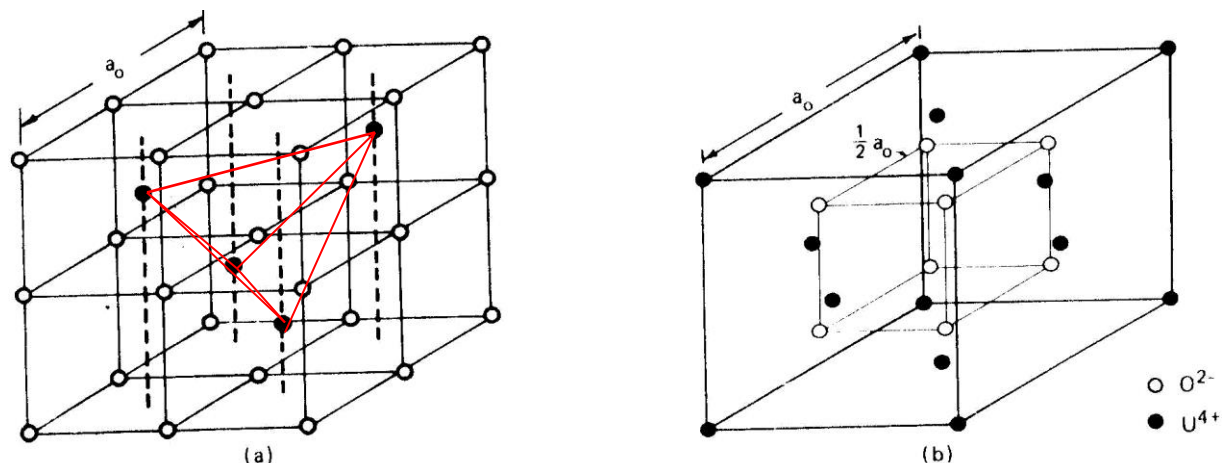


Fig. 3.16 The Fluorite structure of UO_2

Example #6 Theoretical density of UO_2

The lattice parameter of UO_2 is $a_o = 0.547 \text{ nm}$. Thus the volume of the unit cell shown in Fig. 3.15 is 0.164 nm^3 . The unit cell contains 4 uranium atoms and 8 oxygen atoms (each unit cell has to be stoichiometric). The total weight of the atoms within the unit cell is

$$w = \frac{(238 + 2 \times 16)}{6 \times 10^{23}} = \frac{270 \times 4}{6 \times 10^{23}} = 1.79 \times 10^{-21} \text{ g}$$

Thus the theoretical density of UO_2 is $1.79 \times 10^{-21} / 0.164 \times 10^{-21} = 10.95 \text{ g/cm}^3$.

3.7.3 The corundum structure

Another common binary crystal type is the *corundum*, named after its best-known representative, alumina. Corundum structures are restricted to compounds with the generic formula M_2O_3 . These compounds are also called *sesquioxides*. The cation valence is always 3+. The basic feature of this lattice are the large O^{2-} ions, which form an hcp structure of the type shown in Fig. 3.8. Figure 3.17 shows one basal plane of the corundum lattice viewed along the c axis. The superimposed hexagons highlight this familiar pattern. Placement of the Al^{3+} ions in this plane can be viewed in two ways. First, the cations occupy two of the interstices in the close-packed O^{2-} plane; second, the cations form a hexagonal basal plane of the graphite structure (Fig. 3.12).

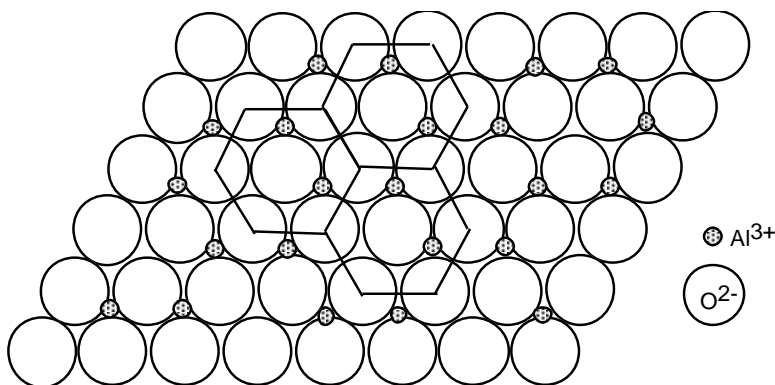


Fig. 3.17 Top view of the corundum unit cell

The hexagons drawn in Fig. 3.17 can be regarded as two-dimensional unit cells of the corundum structure. Each hexagon contains two Al^{3+} entirely within its boundary. Each of the six anions that form the periphery of the hexagons are shared among three such units, so that two peripheral O^{2-} are assigned to each hexagon. Together with the central anion, the planar unit cell contains three oxygen ions. The stoichiometry of the crystal is thus Al_2O_3 , as required.

The complete three-dimensional unit cell of corundum contains six close-packed O^{2-} planes arranged in the stacking sequence of the hcp lattice. Each of these planes is differentiated by the placement of the pairs of cations, which occupy sequentially the six possible adjoining interstitial positions in the hexagon of anions.

In addition to Al_2O_3 , the corrosion products of steel, Cr_2O_3 and Fe_2O_3 , exhibit the corundum lattice structure.

3.7.4 Zirconia

The oxide of zirconium (ZrO_2 or zirconia) is of interest for the purposes of this book, because it is the corrosion product of zirconium-alloy cladding material for nuclear reactor fuels. The details of ZrO_2 will appear in subsequent chapters, and here we are restricted to showing its three lattice types (Fig. 3.18).

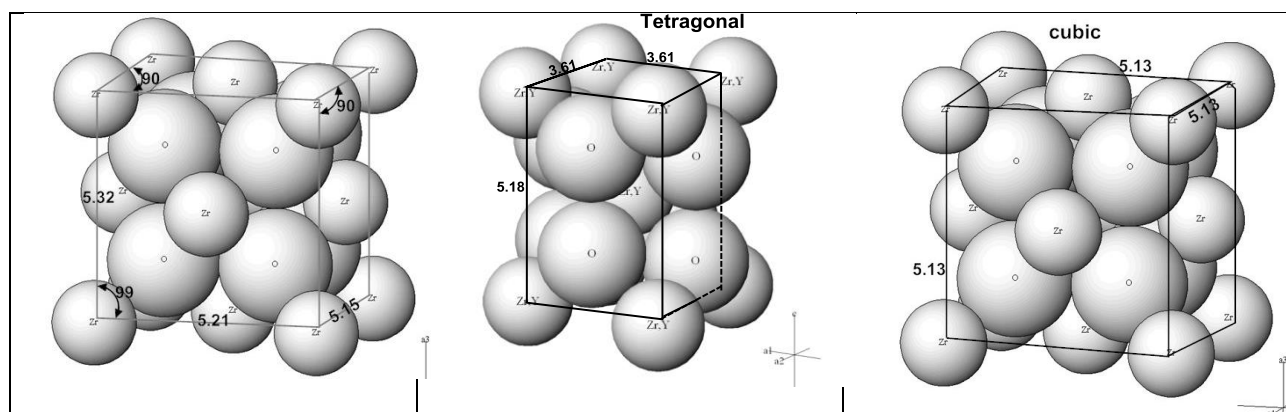


Fig. 3.18 Crystal structures of zirconium dioxide (a) monoclinic, (b) tetragonal and (c) cubic (lattice spacings in Å are shown)

All three structures are part of the fluorite system, but only *cubic* zirconia exhibits a crystal structure that (except for size) is the same as UO_2 (Fig. 3.16). The Zr^{4+} ions rest in face-centered positions and the O^{2-} ions form a simple cubic sublattice inside the cation sublattice.

The *monoclinic* structure exhibits two right angles, but the third is 99° . All three sides are unequal, but not by much. This crystal is the stable form of zirconia up to 1000°C , at which

temperature it transforms to the *tetragonal* variant. The structure of this form is a regular parallelepiped: all angles are 90° , two sides are equal but the third side is larger than the other two. It converts to the cubic structure at 1300°C .

3.7.5 Oxide structures with two cations

Compounds with the general formula $A_xB_yO_z$, where A and B are different cations, are common in mineralogy. Figure 3.19 shows three common structures of this type: *perovskite* (ABO_3), *spinel* (AB_2O_4) and *Scheelite* (ABO_4). A restriction on the two cations is that their valences, weighted by their stoichiometric ratios must balance the charges on the oxygen ions. Perovskite and Scheelite occur in nuclear technology as the so-called *gray phase* in irradiated UO_2 and $(\text{U,Pu})\text{O}_2$ nuclear fuels (Chap. 20). Perovskite is also the crystal structure of some proposed nuclear waste forms.

Oxides with the general formula of AB_2O_4 are called *spinel*s. In this class of oxides, A is a divalent cation and B is normally trivalent. Important members of this group are:

NiCr_2O_4
(nickel chromite)

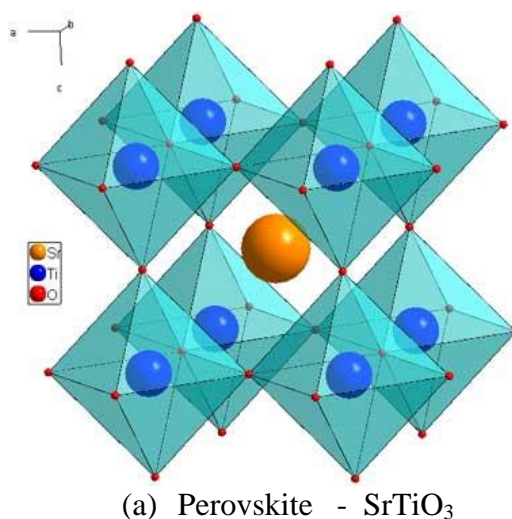
NiFe_2O_4
(nickel ferrite)

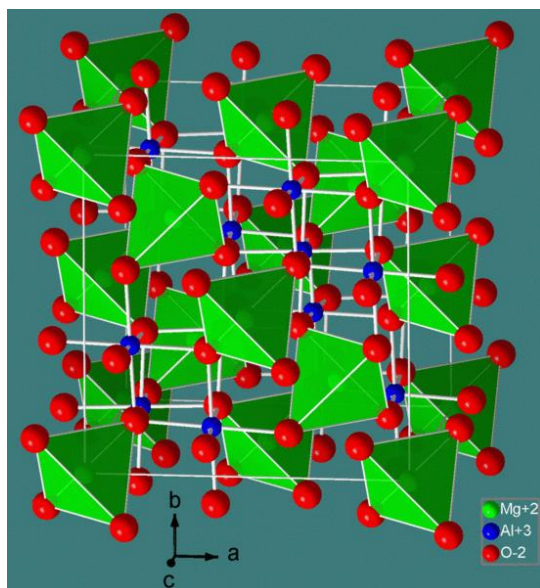
FeCr_2O_4
(ferrous chromite)

FeFe_2O_4
(magnetite)

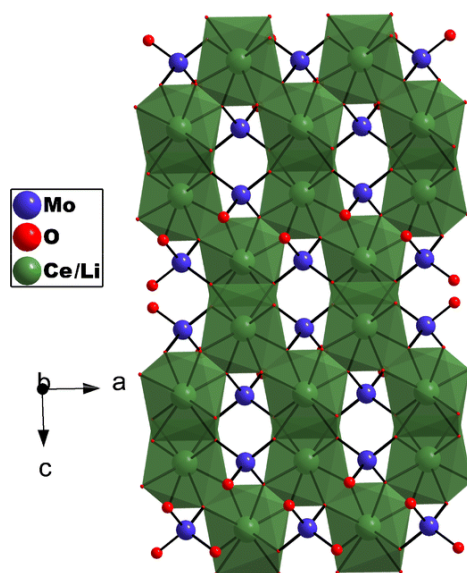
Figure 3.19 shows three of the (111) planes formed by O^{2-} ions in the spinel structure, here exemplified by NiFe_2O_4 . The analysis below shows that the structure diagrams are consistent with the atom ratios $\text{Fe/Ni} = 2$ and $\text{O/Ni} = 4$.

NiFe_2O_4 forms a corrosion layer termed CRUD on Zircaloy cladding and, along with Fe_3O_4 (magnetite), on the stainless steel and Alloy 600 piping in the primary coolant circuit (Chap. 21).





(b) Spinel - MgAl_2O_4



(c) Scheelite - CeMoO_4

Fig. 3.19 Two-cation oxides

3.8 Experimental determination of crystal structure

Knowledge of the crystal structure of materials comes mainly from the coherent scattering of x-rays by crystals. Bragg's law of diffraction establishes a condition for constructive interference from two adjacent atomic planes, which occurs if their path differences are equal to an integral number of wavelengths. Inspection of Fig. 3.21 shows that the difference in path length is:

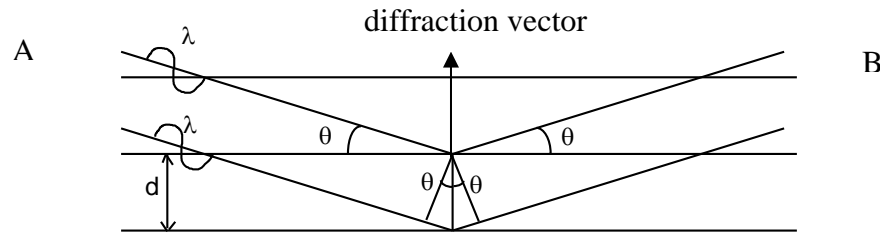


Figure 3.21 Illustration of the Bragg condition for coherent diffraction.

$$n \lambda = 2 d_{hkl} \sin \theta_{hkl} \quad (3.11)$$

where d_{hkl} is the interplanar spacing for plane hkl (Eq (3.5)), θ_{hkl} is the Bragg angle for plane hkl , λ is the wavelength and n is an integer. For every set of planes there is only one angle θ that satisfies the above equation for a given wavelength, so that a given crystallite (a grain) only satisfies the Bragg condition at one angle. With the source at position A and the detector at position B, diffraction can only occur from planes that are perpendicular to the diffraction vector shown in Fig. 3.20. The diffraction vector is defined as the difference between the incident and diffracted beams.

3.8.1. X-Ray diffraction

The standard experiment uses the geometry in Fig. 3.21 and varies θ continuously on a *powder* sample (i.e. one in which there are enough crystallites that some will be oriented perpendicular to the diffraction vector) to sample all the possible peaks within the angular range. The intensities are recorded on a plot of diffracted intensity versus θ as illustrated in Fig 3.22 for hcp Zr. The peak intensities result from the *structure factors* of the samples. In addition to the scattering power of the atoms in the solid, the constructive or destructive interference between waves scattered from the atoms on different crystal planes of the same hkl can lead to variations in the relative peak intensities.

For a perfect crystal the structure factor sums the *scattering power* of the atoms in the unit cell to take into account their mutual constructive or destructive interference. Because the unit cell reflects the symmetry of the lattice, destructive or constructive interference, the structure factor for scattering from the plane (hkl) in direction (xyz) is [5]:

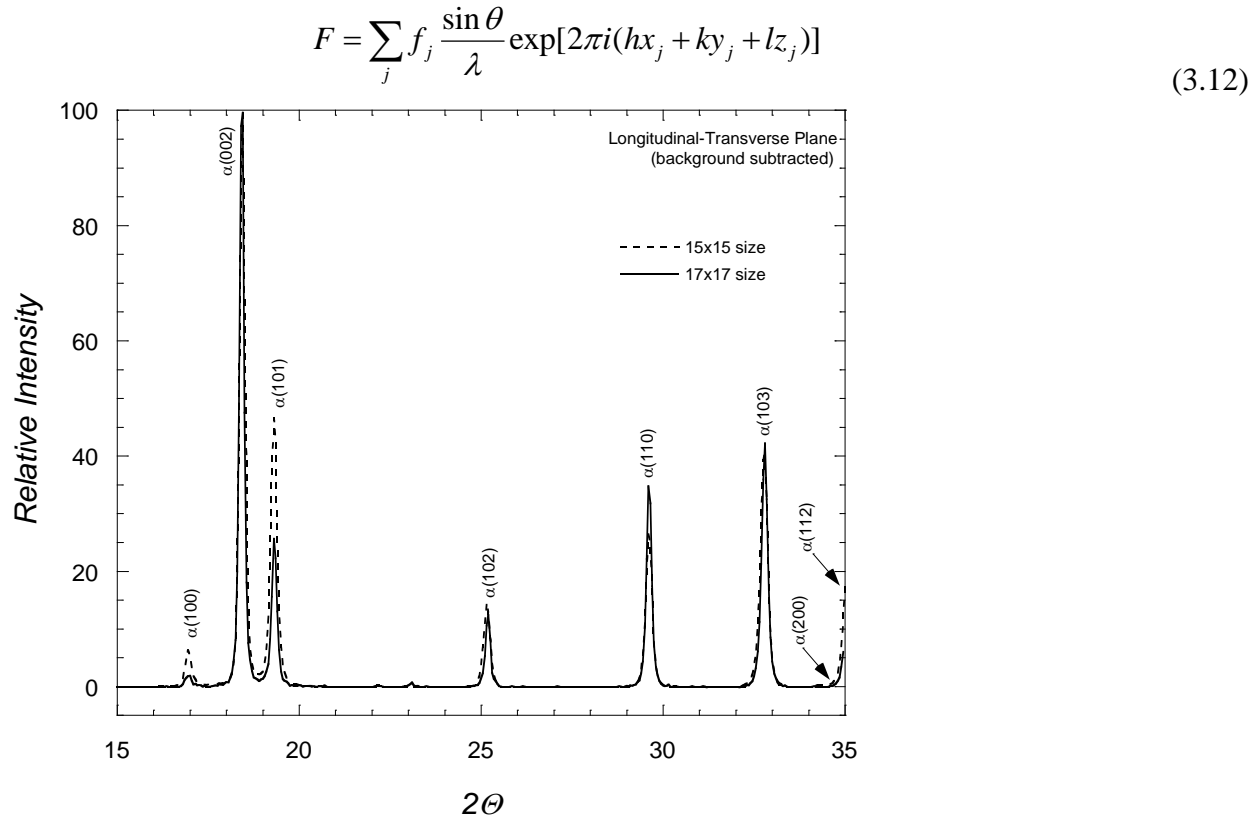


Fig.3.22: X-ray diffraction pattern from two Zircaloy samples with slightly different textures.

where the sum is taken over the all atoms j of the unit cell, and x_j, y_j, z_j , are the fractional coordinates of atom j in the unit cell. $f_j(\sin \theta/\lambda)$ is the atomic scattering factor which includes the overall scattering power of the atom in question (the higher the electron density, the higher the scattering power for x-ray and electron radiation).

The reflections observed in Fig. 3.22 are those for which $F > 0$. Different combinations of hkl with the atom positions in the unit cell give different values of F . A value of $F = 0$ corresponds to extinction of the diffracted beam. In those cases, diffraction from the particular (hkl) plane is said to be *not allowed* for that crystal structure.

An example of extinction is the 100 reflection in the bcc structure. Referring to Fig. 3.5, when constructive interference occurs between the top and bottom planes, the middle plane, lying halfway between the two, represents half the path difference between the x-rays scattered from the top and bottom planes and thus exactly cancels the constructive interference of the (100) planes. Thus no diffracted beam from (100) is possible in the bcc; this is a forbidden reflection.

Example #7 Structure factor in the bcc crystal

The F -factor can also be calculated by considering the bcc unit cell for which the atom coordinates are $(0,0,0)$ and $(\frac{1}{2}, \frac{1}{2}, \frac{1}{2})$. Inserting these positions for $hkl=100$ in Eq (3.12) gives

$$F = f \left\{ \exp[2\pi i(1.0 + 0.0 + 0.0)] + \exp[2\pi i(1. \frac{1}{2} + 0. \frac{1}{2} + 0. \frac{1}{2})] \right\} \quad (3.9)$$

$$F = f[1 + e^{\pi i}] = 0 \quad (3.10)$$

meaning the diffracted intensity of 100 is zero.

For the bcc structure, the only allowed reflections are those for which the sum $h+k+l$ is even, while for fcc, h,k,l need to be all even or all odd. Because of this, the allowed reflections for bcc are (in order of increasing interplanar lattice spacing): 110, 200, 211, 220, 310, 222, etc. For fcc they are 111, 200, 220, 311, 222, 400 etc. For the simple cubic lattice, all reflections are allowed. The rules for hcp are a little more complex but follow the same principle.

In addition to crystal structure parameters, peak intensities and shapes are functions of many instrumental parameters (number of photons, source and detector slit size, energy spread of incoming radiation, distances between detector and sample, electronic noise, etc.). For a given peak in a particular crystal structure, the diffracted intensity depends on:

- the atomic density of the corresponding planes,
- their multiplicity (how many planes of the same type exist),
- the atomic scattering factor of the atom in question,
- the structure factor (how does the scattering from the atoms in the crystal structure combine to produce a scattered signal),
- thermal scattering factors

A good review of these variables is presented in Ref. [6].

The spectra can also be affected by characteristics specific to the sample, such as crystallographic *texture*, the presence of strain, and grain-size effects. The last two cause peak broadening (i.e. the full width at half maximum of each peak increases), and peak shift. The first can result from a sample that exhibits preferential orientation as a result of fabrication processing, as discussed in more detail in Chapter 17 for the case of Zr.

The information gathered in such experiments is available as part of several databases. A spectrum such as Fig. 3.22 is compared to the theoretical values of the intensities for a given crystal structure. These structure determination calculations are involved and make use of modern analysis methods such as Rietveld refinement [7].

3.8.2. Electron Diffraction

The wavelengths of high- energy electrons are small enough that they can interact with lattice planes. Two types of electron microscopes are in common use: a transmission electron microscope (TEM) and a scanning electron microscope (SEM).

The TEM focuses a high-energy (~ 100-400 keV) electron beam on a thin sample (typically less than 200 nm). The beam is partly transmitted through the sample and partly diffracted. Images can be formed from diffraction contrast by an aperture around the transmitted beam after focusing (bright-field image) or around one of the focused diffracted beams (dark-field image).

In a bright-field image, objects that diffract strongly appear dark and in a dark-field image they appear light.

All transmitted and diffracted beams are simultaneously focused on the back focal plane. The image of these focused beams constitutes an *electron diffraction pattern*. An example of such a pattern from a sample of austenite (fcc Fe alloy) is shown in Figure 3.23 (a).

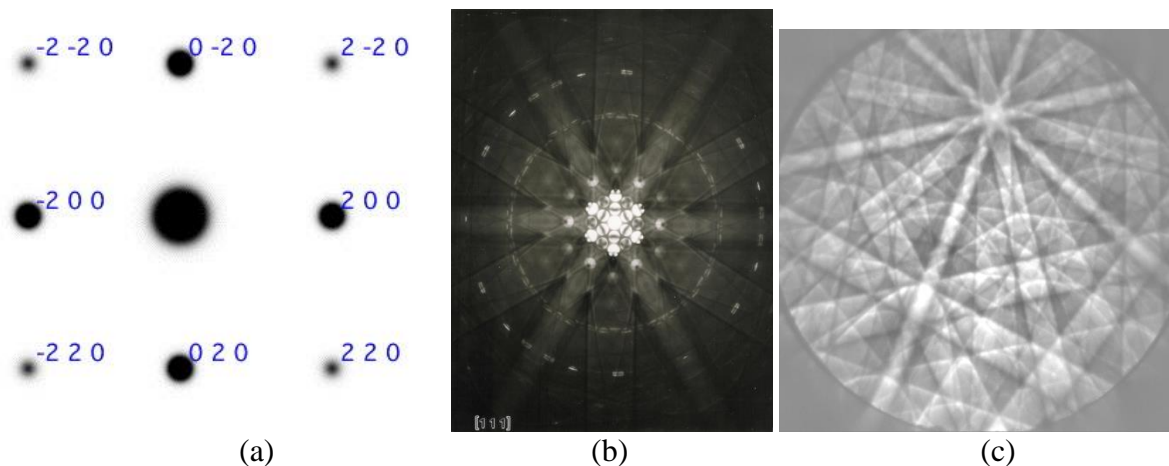


Figure 3.23: Examples of electron diffraction patterns. (a) Electron spot pattern taken using a parallel beam. The large spot in center is the transmitted beam and the smaller spots are diffracted from the various crystal planes in the structure. (b) Convergent beam diffraction pattern of pyrochlore, showing the interference pattern from higher-order Laue zones [8]. ; (c) a Kikuchi pattern, used for orientation imaging (electron backscatter diffraction) and also for proper tilting in the microscope.

The interplanar spacing can be calculated from the diffraction pattern from the formula

$$Rd = \lambda L \quad (3.14)$$

where R is the measured distance in the micrograph, λ is the wavelength and L is the camera length, d is the d-spacing for the plane in question. The angles between planes can be measured directly from the figure. For example the angle between the 220 and $\bar{2}20$ planes is 45 degrees.

Each spot in Fig. 3.23 corresponds to the diffracted electron waves from one set of planes. Because the electron diffraction angle is very shallow (θ small), it is possible to excite simultaneously diffraction from many beams. This pattern of electron diffraction reveals the crystal symmetry better than in x-ray diffraction. In addition, because the electron beam can be focused on a region as small as a few nm, the spatial resolution of transmission electron microscopy diffraction is much higher than that of x-ray diffraction.

However, in general the crystal lattice parameter determinations from TEM are less precise than those obtained with x-ray diffraction because of the larger volume sampled by the latter, and because of the greater precision in measuring angles and distances.

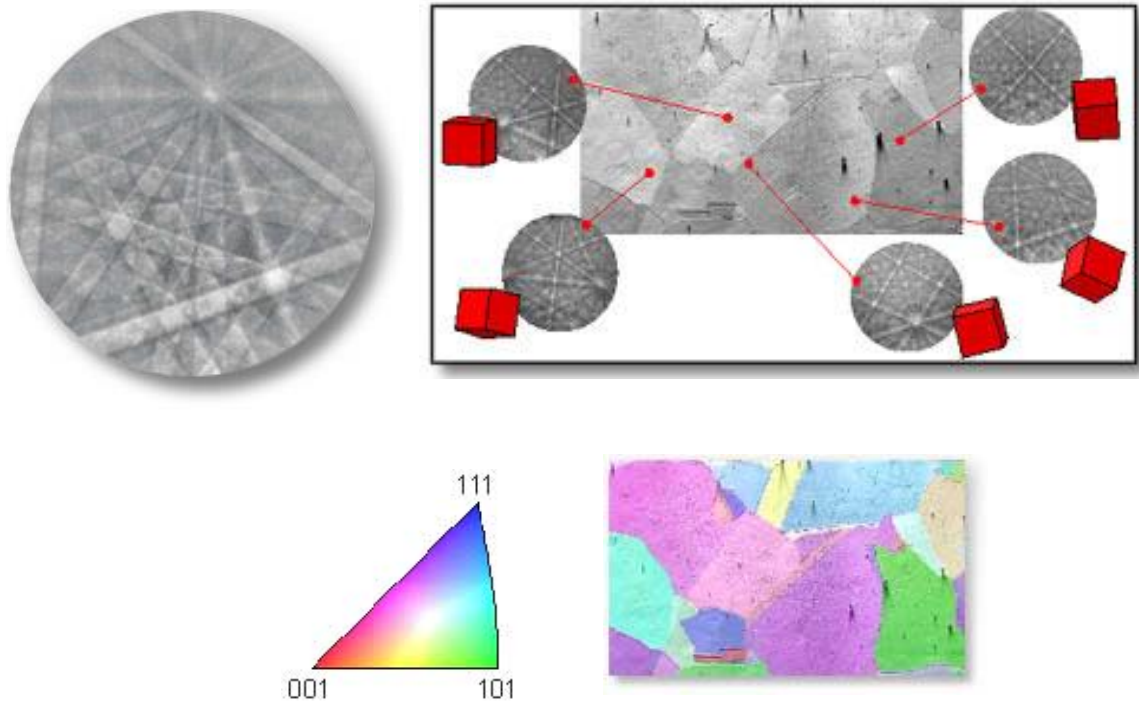


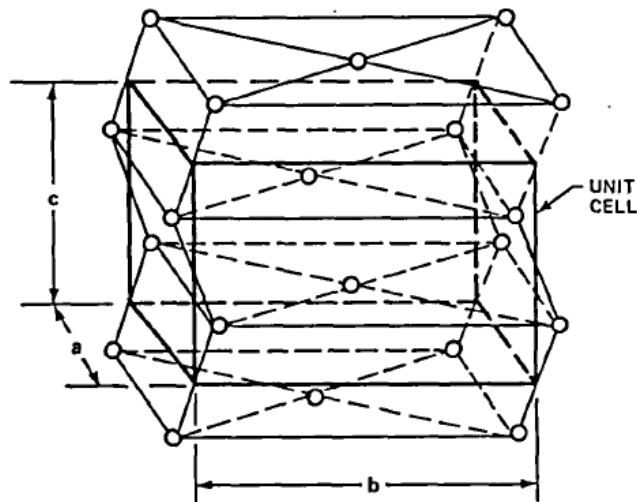
Figure 3.24: Electron backscatter Diffraction Orientation Imaging. The electron beam is scanned across the sample and grains are indexed according to the backscattered Kikuchi lines generated and colored according to their position in the orientation triangle.

The technique of *electron backscattered diffraction* allows diffraction information to be obtained with the *scanning electron microscope* (SEM). The orientation of individual grains can be identified from the diffraction patterns and a much more extensive survey performed of the orientation distribution of grains in a sample than would be possible with the TEM. This allows the identification of grain-to-grain misorientations and strain partitioning between grains. In figure 3.24 for example the color of the grains indicates that not many grains are oriented with the 001 plane parallel to the surface.

Problems

3.1 The crystal structure of α -uranium is shown in the sketch below.

- (a) What is the complete designation of this crystal structure?
 (b) One criterion for the suitability of a nuclear fuel is the uranium atom density. Calculate this parameter and the theoretical atom density for the three nuclear fuels α -uranium, UO_2 and UC. The lattice constants for UO_2 and UC are 0.547 nm and 0.4961 nm, respectively.



CRYSTAL AXIS VECTORS	
DIRECTION	LENGTH, Å
a [100]	2.852
b [010]	5.865
c [001]	4.945

3.2. For a tetragonal lattice where $a=b=3c$, find the indices of the direction perpendicular to the (011) plane.

3.3. If atoms are considered as contacting hard spheres, show that:

- the bcc lattice has a packing fraction of 0.68
- the fcc and hcp lattice have a packing fraction of 0.74
- the hcp structure has $c/a = 1.633$

3.4. Using the hard sphere premise, if a cube has side a_0 what is the atomic diameter in bcc and fcc?

3.5. What low-index crystal planes in the tetragonal systems have the hkl direction perpendicular to the hkl plane?

3.6. Given a bcc structure formed by the packing of hard spheres, what is the largest sphere that can be introduced into the lattice without distortion and where is it located? Such simple geometrical arguments often predict the position of interstitial atoms.

3.7. For the cubic system show that

$$d_{hkl} = \frac{a}{\sqrt{h^2 + k^2 + l^2}}$$

3.8 For the two-dimensional case, show that the choice of primitive unit cell is not unique but that all choices have the same area (volume for 3D case). (Fig. 3.2)

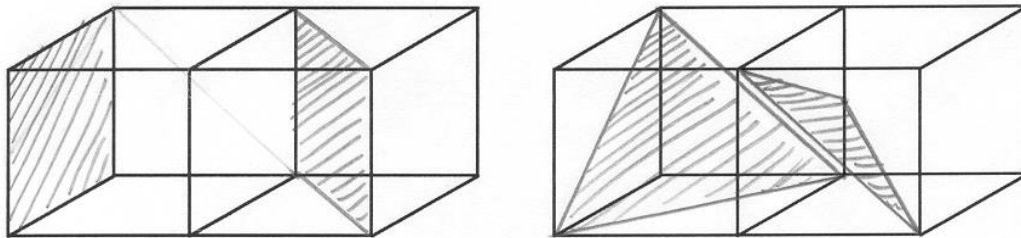
3.9. A cubic crystal lattice parameter is $a_o = 0.36$ nm . Write an expression for a lattice vector from an atom at the origin to one two cells away along the a-axis, 4 cells along the b axis, 6 cells along the c-direction. What is the length of the vector and what angles does it make with the three crystal axes?

Repeat for a monoclinic crystal where $a = 0.2$ nm, $b = 0.36$ nm and $c = 0.24$ nm

3.10. In a simple tetragonal crystal the unit cell dimensions are $a = b = 0.18$ nm and $c = 0.24$ nm Find the spacing between adjacent (111) planes and adjacent (523) planes in the crystal. For the same crystal structure, find the distance between adjacent atoms along the [111] direction and along the [523] direction.

3.11. The conventional unit cell of NaCl (common salt) is shown in Fig. 3.14. What is its crystal structure? How many nearest neighbor atoms do the Cl atoms have and of what type are they?

3.12. What are the Miller indices of the cubic and tetragonal planes below?



References

- [1] C. Kittel, *Introduction to Solid State Physics*, 6th edition: Wiley, (1986).
- [2] J. Edington, *Practical Electron Microscopy in Materials Science*, (1976).
- [3] T. Hahn, *International Tables for Crystallography, Volume A: Space Group Symmetry*, 5th ed ed. Berlin, New York: Springer-Verlag, (2002).
- [4] F. Laves, "Factors governing structure of intermetallic phases," *Advances in X-Ray Analysis* **6** (1963) 43-61.
- [5] G. Thomas and M. J. Goringe, *Transmission Electron Microscopy of Materials*. New York: John Wiley and Sons, (1979).
- [6] B. Cullity, *Elements of X-ray Diffraction*. Reading, MA: Addison-Wesley, (1978).
- [7] R. Young, *The Rietveld Method*: Oxford: University Press, (1993).
- [8] A. Landa-Cánovas, L. C. Otero-Díaz, L. Botto, and I. B. Schalamuk, "Electron microscopy study of the decomposition products at 1300°C from jamesonite mineral $\text{FePb}_4\text{Sb}_6\text{S}_{14}$," *Solid State Ionics* **63-65** (1993) 301-306.